Benchmarking the Molecular Mechanics−Valence Bond Method: Photophysics of Styrene and Indene

Michael J. Bearpark,[†] Fernando Bernardi,[‡] Massimo Olivucci,*[,‡] and Michael A. Robb*[,†]

Dipartimento di Chimica 'G. Ciamician' dell' Universitá di Bologna, Via Selmi 2, 40126 Bologna, Italy, and Department of Chemistry, King's College London, Strand, London WC2R 2LS, U.K.

Received: May 29, 1997; In Final Form: August 18, 1997[⊗]

We have recently studied the excited states of the simplest aryl olefin styrene (Bearpark, M. J.; Olivucci, M.; Wilsey, S.; Bernardi, F.; Robb, M. A. *J. Am. Chem. Soc.* **1995**, *117*, 6944−6953) at the CASSCF / 4-31G level of theory. Full geometry optimization was shown to be essential in characterizing decay funnels for internal conversion (activated) and intersystem crossing (activationless) processes in this molecule. Here, we demonstrate that the CASSCF potential energy surfaces for styrene excited states can be simulated to an acceptable level of accuracy using a hybrid molecular mechanics−valence bond method (MMVB), which is many orders of magnitude less expensive computationally than CASSCF. The nonradiative deactivation of styrene and indene from S_1 is compared. Because ethylene torsions are restricted, the mechanism proposed for styrene S_1 decay (involving S_1/T_2, T_2/T_1, and T_1/S_0 surface crossings) is much less likely to occur in indene. The existence of both S_2/S_1 and S_1/S_0 conical intersections is consistent with the lack of fluorescence observed after exciting indene to S_2 in the gas phase and suggests that rearrangement reactions may be due to vibrationally excited S_0*.

Introduction

The photophysics of aryl olefins such as styrene **1**,[1] stilbene,[2]

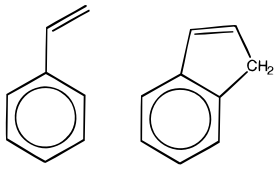

1 **2**

α,ω-diphenylpolyenes,[3] and tetraphenylethylene[4] has been studied using time-resolved spectroscopic techniques, and differences in excited state behavior have emerged that cannot be accounted for using the standard model of decay at a perpendicular funnel.[5] For example, the $S_1 \rightarrow S_0$ decay of *cis*-stilbene can take place in less than 150 fs,[2b] a factor of $\sim 1 \times 10^5$ faster than in styrene,[1b] which suggests that the respective potential energy surfaces have a markedly different topology.

Previous theoretical investigations—semiempirical[6] and ab initio[7]—were limited by the fact that full geometry optimization of critical points on excited-state potential energy surfaces could not be carried out. Recent CASSCF work has demonstrated the importance of relaxing geometric constraints,[8] particularly in the search for unavoided surface crossings (conical intersections[9]) at which decay can be fully efficient.[9m] For example, calculations for the H_4 system[10] anticipated the location of S_1/S_0 surface crossings in ethylene + ethylene (rhomboidal geometry[8a,b]) and butadiene (twisted perpendicular geometry[8d]). Decay at a pericyclic minimum had previously been assumed,[11] although the energy gap at such a geometry in butadiene is ∼70 kcal mol^{-1}.

In the case of styrene[1,12−18] we have recently demonstrated[8i] that changes in bonding within the benzene ring following excitation cannot be neglected,[5] as the two mechanisms for S_1 decay set out in Scheme 1 (where **1a**, **1b**, **1g**, **1h**, and **1m** refer to optimized geometries of Figure 1 that we shall discuss subsequently) show. The lowest energy pathway to efficient internal conversion (IC) is via an S_1/S_0 conical intersection that results from a distortion of the benzene ring alone[8h] (Scheme 1, left). Decay at this point is an activated process; a vibrational excess energy of ∼3000 cm^{-1} is required, the same as that for the "channel 3", which precludes S_1 fluorescence in benzene.[19] No cis−trans isomerization is detected experimentally at these energies.[12a] Alternatively (Scheme 1, right), with little vibrational excess energy, intersystem crossing (ISC)[1,13] competes with fluorescence[14] because S_1 and T_2 are approximately degenerate in the region of the S_1 planar minimum. Decay from S_1 to T_2 is followed by fast T_2/T_1 IC, leading to ISC in the region of the twisted minimum on T_1 where S_0 is approximately degenerate and cis−trans isomerization can occur. In addition, adiabatic cis−trans isomerization can take place on S_1 at intermediate excess energies, but IC at a twisted minimum[5] (not shown in Scheme 1) is unlikely because the $S_1 \rightarrow S_0$ energy gap is so large (∼70 kcal mol^{-1} [8i]).

SCHEME 1

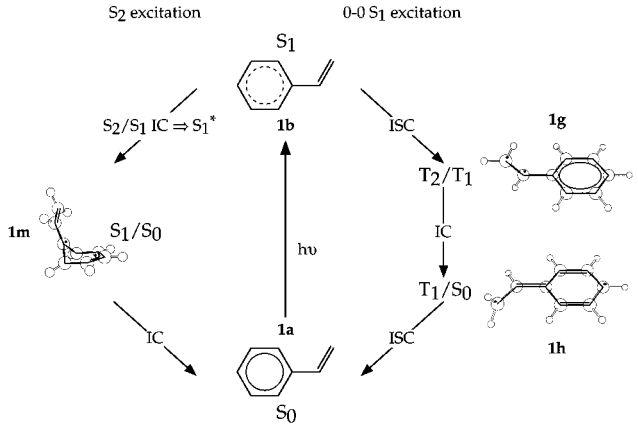

Full geometry optimization at the CASSCF/4-31G level of theory was essential in characterizing the structures along both

† King's College London.
‡ 'G. Ciamician' dell' Universitá di Bologna.
⊗ Abstract published in *Advance ACS Abstracts,* October 1, 1997.

S1089-5639(97)01733-7 CCC: $14.00

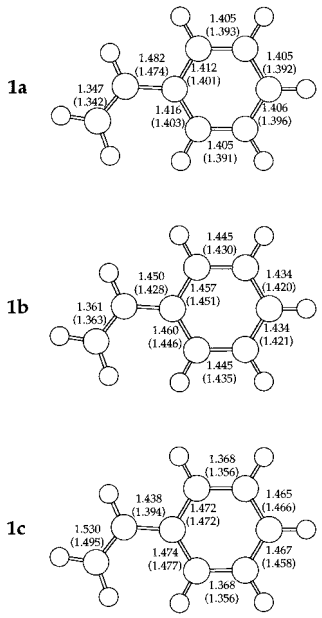

Figure 1. Styrene: relaxed MMVB planar singlet structures on S_0 (**1a**), S_1 (**1b**), and S_2 (**1c**). All bond lengths are in angstroms. CASSCF/4-31G measurements are from ref 8i in parentheses. Energies are in Table 1.

reaction paths for styrene[8i] shown in Scheme 1. Ethylene torsion without ring relaxation was insufficient (cf. ref 1). However, such calculations are not yet practical for aryl olefins with two or more aromatic rings because of the large number of electrons that must be correlated. For this reason, we have developed the molecular mechanics−valence bond (MMVB) method,[20] which can be used to simulate CASSCF/4-31G calculations for covalent states of conjugated hydrocarbons inexpensively. MMVB has previously been used in conjunction with CASSCF to model the decay dynamics of benzene,[19] fulvene,[8k] and azulene[8j] and to predict the existence of a benzene-like conical intersection in [18]annulene.[8l] In this paper, the aim is to show that the topology of the covalent excited states of styrene determined with MMVB and CASSCF is the same and that the mechanisms for excited-state decay (Scheme 1[8i]) are reproduced quite well from MMVB calculations alone. MMVB is therefore a useful tool for predicting the behavior of the excited states of larger aryl olefins, where CASSCF calculations are presently impractical. As an illustration, we use MMVB here to contrast the behavior of the excited states of styrene and indene **2**[21−25] in which the additional $-CH_2-$ group hinders ethylene torsion. The consequences of this constraint for the decay of S_1 indene are evaluated.

Computational Details

MMVB[20] is a hybrid method that uses the MM2 potential[26] to describe an inert molecular σ-framework. Active electrons—those involved in conjugation and new σ-bond formation—are represented by a Heisenberg Hamiltonian[27] in the space of neutral valence bond configurations. Because of this, MMVB can only describe covalent states, which for styrene means that the twisted ionic minimum labeled **k** in ref 8i cannot be considered here. This intermediate is not directly involved in S_1 decay[1,7b,8i] but may be responsible for the dual fluorescence of styrene that can be observed.[12] Ionic contributions are not neglected completely in MMVB; their effect is included by virtue of the parametrization against CASSCF computations.[20] The S_1/S_0 gap for the covalent twisted minimum labeled **f** in ref 8i may nevertheless be overestimated.

A general set of molecular VB parameters (derived from CASSCF/4-31G calculations) are presently available for sp^2/sp^3 carbon atoms. Energies and analytical gradients can be calculated for the ground and valence excited states of systems with up to 24 carbon active sites.[20b] Such computations take a few seconds for styrene and indene (with 8 active sites) on current RISC workstations. Minima on conical intersections[9] are optimized using the algorithm described in ref 28b. In the case of a singlet−triplet crossing, the intersection space[9l] has the dimension $(n - 1)$, since the derivative coupling is zero between states of different spin multiplicity. The branching space (in which initial motion on the lower state will take place) is therefore one-dimensional[20b,8i] in this case.

We consider two mechanisms for radiationless decay in this paper. When real surface crossings exist and are accessible, the Landau−Zener model[9h] provides a semiclassical model for fast radiationless decay. By "accessible", we mean that there is a reaction coordinate with a sufficiently low-energy barrier that leads from the initial excited-state geometry to the crossing region. In azulene,[8j] for example, the initial in-plane motion on S_1 is strongly directed toward an S_1/S_0 intersection and there is no intervening transition structure. Radiationless decay at such a crossing is consistent with the observed S_1 lifetime of $\ll$1 ps.[32] If surface crossings are not present, or are present but not easily accessible, the process of radiationless decay may be better described as the transformation of electronic energy into a manifold of vibronic states associated with the lower electronic state. This process is governed by the density of states and Franck−Condon factors according to the Fermi golden rule formalism. As the energy gap gets larger the density of states gets larger but the Franck−Condon factors become unfavorable.

As shown by Desouter-Lecomte and Lorquet,[9p] the probability of radiationless decay is given as

$$P = \exp[-(\pi/4)\xi] \tag{1}$$

where ξ is the Massey parameter given as

$$\xi = \frac{\Delta E(q)}{\frac{h}{2\pi}|\dot{\mathbf{q}}||g(\mathbf{q})|} \tag{2}$$

where $\mathbf{q}$ is a vector of nuclear displacement coordinates. The term $g(\mathbf{q})$ is the nonadiabatic coupling matrix element defined as

$$g(\mathbf{q}) = \left\langle \Psi_1 \left| \frac{\partial \Psi_2}{\partial \mathbf{q}} \right\rangle \right. \tag{3}$$

while $|\dot{q}|$ is the magnitude of the velocity along the reaction path $\mathbf{q}$ and ΔE is the energy gap between the two states Ψ_1 and Ψ_2. Unless ΔE is less than a few kJ mol^{-1}, the decay probability predicted in this model[9h] is vanishing small. However, as we approach a point where the surfaces actually cross, the decay probability becomes unity. If real crossing points exist and are accessible (see ref 8 for many examples), decay at these points should predominate over the transformation of electronic to vibrational energy via the Fermi golden rule formalism when an energy gap is present. Associated with this process the energy gap law (see p 76 of ref 9r), which for internal conversion has the form

$$k_{IC} \cong 10^{13} \exp\{-4.5\Delta E_{S_1-S_0}\} \tag{4}$$

and typical IC rates for aromatic hydrocarbons are found to be 10^5-10^6 s^{-1} (ref 9s, p 130).

TABLE 1: Styrene MMVB Energies/E_h (Top Line) at MMVB Optimized Geometries[a]

structure	S_0	T_1	T_2	S_1	S_2
1a, M,[b] S_0	−0.44270	−0.35747	−0.29075	−0.28656	−0.21719
	−93.3	−39.9	2.0	4.6	48.2
	(−104.7)	(−28.5)	(−2.9)	(5.6)	(46.2)
1b, M, S_1	−0.43501	−0.36025	−0.29504	−0.29394	
	−88.5	−41.6	−0.7	0.0	
			(−4.8)	(0.0)	
1c, M, S_2	−0.40863			−0.26359	−0.26079
	−72.0			19.0	20.8
					(21.2)[e]
1d, M, T_1		−0.36558			
		−45.0			
		(−41.6)			
1e, M, T_2		−0.35172	−0.31073		
		−36.3	−10.5		
			(−10.3)		
1f, X,[c] S_1/T_2	−0.35770	−0.35768	−0.27161	−0.27161	
	−40.0	−40.0	14.0	14.0	
	(−59.0)[d]		(15.2)	(17.0)	
1g, X, T_1/T_2		−0.31752	−0.31664		
		−14.8	−14.2		
		(−11.5)	(−10.5)		
1h, X, S_0/T_1	−0.36612	−0.36610			
	−45.3	−45.3			
	(−48.3)	(−47.6)			
1j, X, S_0/T_1	−0.26581	−0.26578			
	17.7	17.7			
	(3.9)	(3.2)			
1l, X, S_0/S_1	−0.24862			−0.24742	
	28.4			29.2	
	(42.3)			(43.7)	
1m, X, S_0/S_1	−0.24467			−0.24457	
	30.9			31.0	
	(24.6)			(28.2)	

[a] Styrene MMVB geometries are shown in Figures 1−7. Energies are relative to the styrene planar S_1 minimum **1b**/kcal mol^{-1} (middle line). Relative energies are calculated at the CASSCF/4-31G level for optimized geometries taken from ref 8i /kcal mol^{-1} (bottom line). [b] M = planar minimum. [c] X = surface crossing. [d] 6-31G* value.[8i] [e] Further optimization at CASSCF/4-31G level[8i] leads to a slightly twisted S_2/S_1 intersection with roots 19.0 (S_0) and 22.0 (S_1) kcal mol^{-1} above the S_1 planar minimum **1b**.

The results of ab initio CASSCF/4-31G geometry optimizations for styrene have already been published.[8i] For comparison in this study, planar structures were optimized for the S_0 and S_1 states of indene at the CASSCF/3-21G level. The same active space of eight electrons in eight π-orbitals was used for styrene and indene. Analytical frequency calculations were carried out at both indene geometries to establish that they are energy minima. (The frequencies have been published elsewhere.[30])

Results and Discussion

The MMVB structures for styrene **1** and indene **2** presented here will be labeled sequentially **a**−**m** (following the notation used in ref 8i).

Styrene. All of the minima and conical intersections **a**−**m** previously characterized for the valence excited states of styrene with CASSCF[8i] have been located with MMVB. The CASSCF and MMVB optimized geometries, the gradient of T_2 at the S_1/T_2 crossing, and the gradient difference at the T_2/T_1 conical intersection are collected in Figures 1−7. In Table 1 we give the energies of S_0, T_1, T_2, S_1, and S_2 for the optimized geometries **a**−**m**. MMVB reproduces the CASSCF ordering of states at each point, and the relative energies—apart from structures with puckered benzene rings such as **1j**, **1l**, and **1m**—differ only by ±10% or so. Experimentally, the S_2 and S_3 bands overlap.[16] One is ionic,[6a,b] the other is a valence state with ionic character similar to the S_2 state of benzene.[8h] (S_1 is L_b and S_2 is L_a in the Platt notation). MMVB was parametrized from CASSCF/4-31G calculations, and it appears from Table 1 that both methods overestimate the relative energies for styrene S_2 equally.

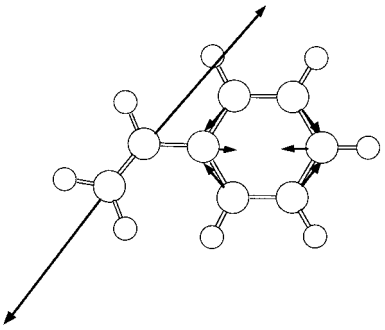

Figure 2. Styrene: MMVB gradient on T_2 at the S_1/T_2 planar crossing **1b**.

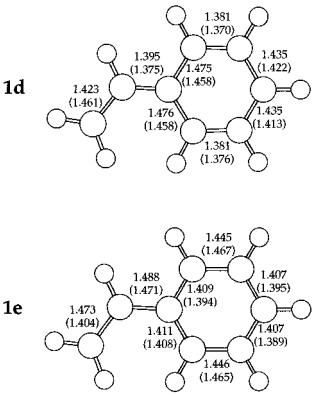

Figure 3. Styrene: relaxed MMVB planar triplet structures on T_1 (**1d**) and T_2 (**1e**). All bond lengths are in angstroms. CASSCF/4-31G measurements are from ref 8i in parentheses. Energies are in Table 1.

Figures 1 and 3 show that the nature of the geometry changes on 0−0 excitation are correctly reproduced by MMVB. In S_1 (**1b**) this involves uniform benzene-like[8h] ring expansion together with a small butadiene-like[14c] increase in ethylene bond length and decrease in the ethylene−benzene bond length. All of these changes have been identified from the sharp absorption and fluorescence spectra[14] of the near-vertical[15a] $S_0 \rightarrow S_1$ transition.

Table 1 shows that the MMVB S_1 and T_2 states are approximately degenerate at **1b**. Since **1b** is a minimum on S_1, it is also a minimum on an $(n-1)$ dimensional S_1/T_2 surface crossing and spin-forbidden decay may eventually take place. This is consistent with the experimental observation that a nonradiative decay path operates in styrene at 77K[13a,b,1a] and that the measured quantum yield for ISC at 298K is ∼0.5.[13c,1b] The MMVB gradient on T_2 at **1b** is shown in Figure 2 and is identical with the CASSCF gradient.[8i] It consists of ethylene expansion and anti-quinoid ring distortion, pointing toward the T_2 minimum **1e**.

The diffuse absorption of S_2[15] suggests that rapid IC to S_1 takes place. MMVB and CASSCF[8i] both find that the S_2 and S_1 states are almost degenerate at the S_2 planar minimum **1c** (Table 1), suggesting that barrierless IC to S_1 can take place after initial excitation to S_2. Subsequent pathways on S_1 lead either to the planar minimum **1b** or a twisted minimum **1f** (Figure 4) with a quinoid ring structure.[5,17] The energy difference between **1b** and **1f** is effectively the barrier height for adiabatic isomerization on S_1 and is 14 kcal mol^{-1} with

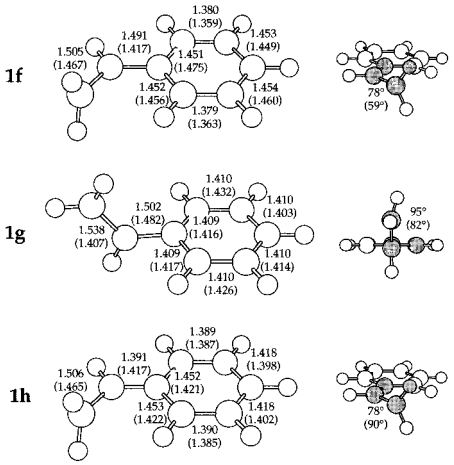

Figure 4. Styrene: MMVB twisted minimum on S_1 (**1f**), T_2/T_1 conical intersection (**1g**), and T_0/S_1 crossing (**1h**). All bond lengths are in angstroms. CASSCF/4-31G measurements are from ref 8i in parentheses. Energies are in Table 1.

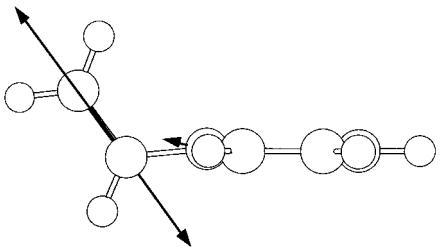

Figure 5. Styrene: MMVB gradient difference vector at the T_2/T_1 conical intersection **1g**.

MMVB and 17 kcal mol^{-1} with CASSCF/4-31G. Both methods show that the $S_1 \rightarrow S_0$ gap at **1f** is too large (see Computational Details section and ref 9h) for IC to be likely at this point (although S_1 and T_2 are degenerate, suggesting that ISC may take place[8i,13c]).

Figure 2 shows that the T_1 and T_2 planar minima are well reproduced at the MMVB level with the exception of the change in ethylene bond length. This may be due to a small imbalance in the parametrization of MMVB when the VB interaction is weak, leading to a bond length nearer to the MM minimum for a C−C single bond. However, both MMVB and CASSCF suggest that **1e** is not the lowest energy point on the T_2 surface, which is instead a T_2/T_1 conical intersection **1g** (Figure 4 and Scheme 1). Both methods find that the derivative coupling and gradient difference vectors are parallel at this geometry, which means that the crossing is effectively $(n - 1)$ dimensional[8i] at this point. The direction that lifts the degeneracy at **1g** is shown in Figure 5; there is no component of rotation about the ethylene or ethylene−benzene bonds but uniform ring and ethylene expansion.

The energy difference between spectroscopic and relaxed T_1 states in styrene is known to be about 10 kcal mol^{-1}.[31a−e] MMVB underestimates this difference but correctly finds a T_1/S_0 crossing **1h** (Figure 4 and Scheme 1) at a perpendicular geometry to be the lowest energy point on T_1. This is consistent with the observed lack of phosphorescence from T_1.[13a,b]

There is an additional T_1/S_0 crossing **1j** similar to the one previously located in benzene,[28b] which is illustrated in Figure 6. Although the MMVB and CASSCF geometries are in good agreement (±0.02 Å), MMVB overestimates the energy of this structure relative to **1b** by 14 kcal mol^{-1} compared with CASSCF. The relative energy of the S_1/S_0 intersections **1l** and **1m** are also overestimated by a similar amount, although the geometries are good. MMVB overestimating CASSCF energies

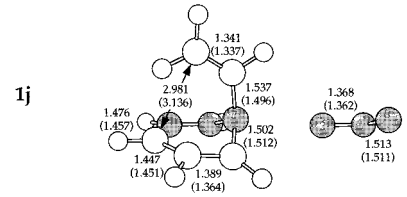

Figure 6. Styrene: MMVB benzene-like T_1/S_0 intersection **1j**. All bond lengths are in angstroms. CASSCF/4-31G measurements are from ref 8i in parentheses. Energies are in Table 1.

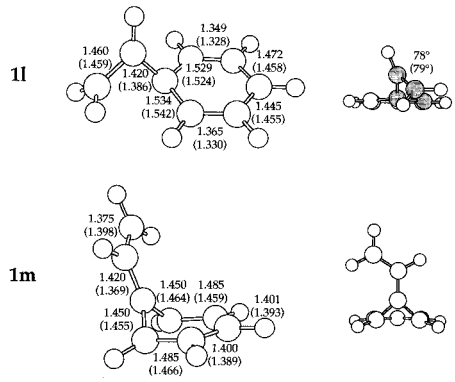

Figure 7. Styrene: MMVB S_1/S_0 conical intersection structures **1l** and **1m**. All bond lengths are in angstroms. CASSCF/4-31G measurements are from ref 8i in parentheses. Energies are in Table 1.

points to a deficiency in part of the parametrization, but the CASSCF values themselves for **1j**−**1m** are also overestimates; in benzene, the energy difference between planar S_1 minimum and S_1/S_0 conical intersection resembling **1m** was calculated to be 23 kcal mol^{-1} with CASSCF/4-31G, compared with the experimental activation energy of 8 kcal mol^{-1} (3000 cm^{-1}).

Indene. Indene **2**[21−25] and styrene **1** contain the same chromophores, but in the former the C═C bond is prevented from twisting by being incorporated into a five-membered ring. This leads to qualitative differences in the photochemical decay mechanisms (aside from the possibility of rearrangement in indene).

The MMVB planar singlet and triplet indene structures **2a**−**2e** illustrated in Figures 8−10 show very similar structural changes to styrene **1a**−**1e** on excitation. (CASSCF computations have been performed only for the S_0 and S_1 minima.) The vertical nature of the $S_0 \rightarrow S_1$ transition is consistent with structured absorption/fluorescence and the observation of the 0−0 band at 77 K.[13a] Structure **2b** is a minimum on S_1[30] and also a minimum on the S_1/T_2 intersection with a gradient on T_2 (Figure 9) identical with that of styrene (Figure 2).

As with styrene, decay from S_1 to T_2 may compete with fluorescence. In indene, however, the T_2/T_1 conical intersection **2g** is over 22 kcal mol^{-1} above **2b**, whereas **1g** is 14 kcal mol^{-1} below **1b** in styrene. This is a result of twisting in the five-membered ring being hindered, which must be offset by an antiquinoid ring distortion leading to crossing at a much higher energy on the T_2/T_1 intersection seam. Accelerated $T_2 \rightarrow T_1$ decay via such a crossing is therefore unlikely in indene, and the Fermi golden rule is a better description of this process. The derivative coupling and gradient difference vectors at **2g** are illustrated in Figure 12 and are no longer parallel as in styrene (**1g**). Because ethylene twisting is suppressed, no twisted S_1 minimum[5] could be located in indene. Searches for a twisted S_1/T_2 crossing resembling **1f** always led the planar S_1/T_2 crossing **2b**.

The planar structure **2d** is the lowest energy point on the indene T_1 surface. This is consistent with the fact that the

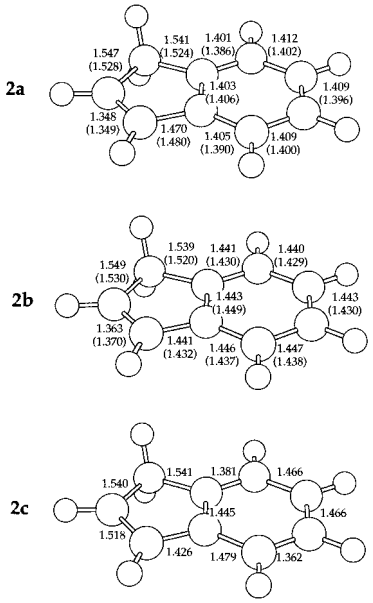

Figure 8. Indene: relaxed MMVB planar singlet structures on S_0 (**2a**), S_1 (**2b**), and S_2 (**2c**). All bond lengths are in angstroms. CASSCF/3-21G measurements in parentheses. Energies are in Table 2.

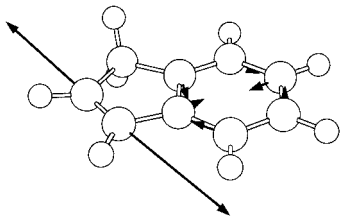

Figure 9. Indene: MMVB gradient on T_2 at the S_1/T_2 planar crossing **2b**.

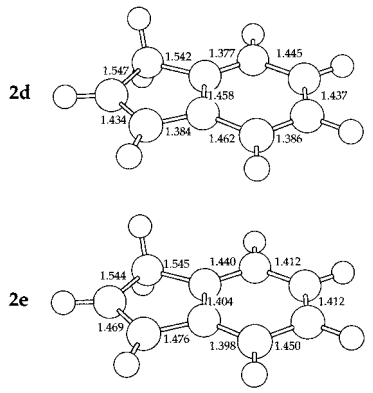

Figure 10. Indene: relaxed MMVB planar triplet structures on T_1 (**2d**) and T_2 (**2e**). All bond lengths are in angstroms. Energies are in Table 2.

spectroscopic and relaxed energies for T_1 are identical,[31a,b] in contrast to styrene. The geometry for ISC via a surface-crossing mechanism—the T_1/S_0 crossing point **2h**—is over 30 kcal mol^{-1} higher in energy and unlikely to be accessible. Caldwell has further shown[31c] that T_1 decay is unaffected by heavy atom substituents and that ISC is inefficient, leading to a microsecond lifetime.

The broad S_2 absorption of indene implies rapid IC to S_1,[24] which accords with the S_2 indene minimum **2c** being a point on the S_2/S_1 intersection (as with styrene). Subsequent rapid S_1/S_0 IC explains the lack of S_1 fluorescence after exciting indene to S_2 in the gas phase,[25] since vibrationally excited S_1 indene can decay at one of four S_1/S_0 conical intersections **2mI**−**2mIV** (Figure 13) resembling **1m**. A conical intersection like

TABLE 2: Indene MMVB Energies/E_h (Top Line) at MMVB Optimized Geometries[a]

structure	S_0	T_1	T_2	S_1	S_2
2a, M,[b] S_0	−0.43267	−0.34699	−0.28184	−0.27609	−0.21382
	−93.8	−40.0	0.9	4.5	43.6
2b, M, S_1	−0.42528	−0.34968	−0.28552	−0.28324	
	−89.1	−41.7	−1.4	0.0	
2c, M, S_2	−0.40199			−0.25618	−0.25549
	−74.5			17.0	17.4
2d, M, T_1		−0.35488			
		−45.0			
2e, M, T_2		−0.34235	−0.30151		
		−37.1	−11.5		
2g, X,[c] T_1/T_2		−0.24843	−0.24670		
		21.8	22.9		
2h, X, S_0/T_1	−0.30392	−0.30389			
	−13.0	−13.0			
2mI, X, S_0/S_1	−0.22078			−0.22077	
	39.2			39.2	
2mII, X, S_0/S_1	−0.22140			−0.22134	
	38.8			38.8	
2mIII, X, S_0/S_1	−0.21827			−0.21825	
	40.8			40.8	
2mIV, X, S_0/S_1	−0.22384			−0.22370	
	37.2			37.4	

[a] Indene MMVB geometries are shown in Figures 8−13. Energies are relative to the indene planar S_1 minimum **2b**/kcal mol^{-1} (bottom line). [b] M = planar minimum. [c] X = surface crossing.

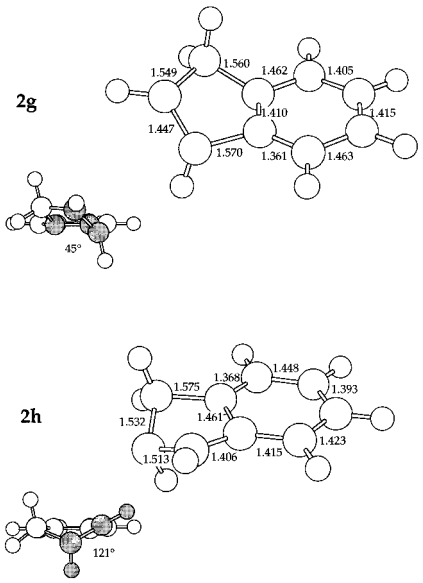

Figure 11. Indene: MMVB T_2/T_1 conical intersection (**2g**) and T_0/S_1 crossing (**2h**). All bond lengths are in angstroms. Energies are in Table 2.

styrene **1l** could not be located for indene. However, such a crossing may be important in the S_1 decay of benzocycloalkadienes with larger rings, e.g., benzocyclooctadiene,[13a] in which the ethylene group is twisted with respect to the ring by an angle approaching 90°, promoting IC.[33]

Conclusion

The topology of the excited-state potential energy surfaces for styrene predicted by MMVB and CASSCF is identical. Both

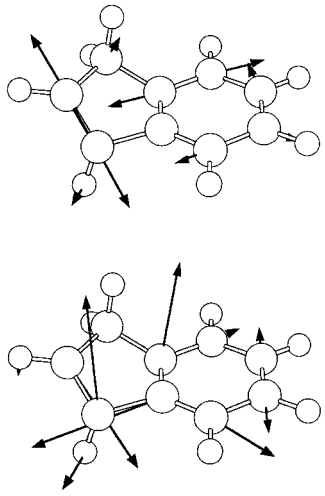

Figure 12. Indene: MMVB derivative coupling (top) and gradient difference (bottom) vectors at the T_2/T_1 conical intersection **2g**.

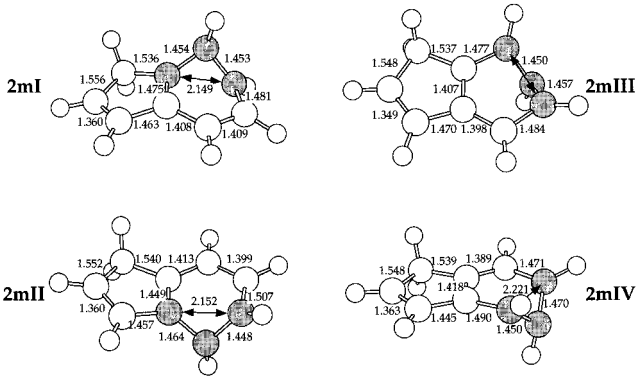

Figure 13. Indene: MMVB S_1/S_0 conical intersection structures **2mI**−**2mIV**. All bond lengths are in angstroms. Energies are in Table 1.

mechanisms set out in Scheme 1 for S_1 decay could have been deduced without CASSCF calculations, which are many orders of magnitude more expensive computationally. In particular, both methods suggest that the energy gap at a twisted S_2-like structure on S_1[5] is too large for IC to be likely.

For indene, the five-membered ring restricts the torsions that are required for the nonradiative deactivation of S_1 via S_1/T_2, T_2/T_1, and T_1/S_0 surface crossings. MMVB predicts that a T_2/T_1 conical intersection is inaccessible. The existence of both S_2/S_1 and S_1/S_0 conical intersections is consistent with the lack of fluorescence observed after exciting indene to S_2 in the gas phase and suggests that rearrangement reactions may be due to vibrationally excited S_0*.

Acknowledgment. This research has been supported in part by the SERC (U.K.) under Grant No, GR/J25123 and GR/H58070. Ab initio computations were run on an IBM RS/6000 using a development version of the Gaussian 94 program.[29]

References and Notes

(1) (a) Lewis, F. D.; Bassani, D. M. *J. Am. Chem. Soc.* **1993**, *115*, 7523−7524. (b) Lewis, F. D.; Bassani, D. M.; Caldwell, R. A.; Unett, D. J. *J. Am. Chem. Soc.* **1994**, *116*, 10477−10485.

(2) (a) Saltiel, J.; Sun, Y.-P. In *Photochromism: Molecules and Systems*; Dürr, H., Bouas-Laurent, H., Eds.; Elsevier: Amsterdam, 1990; pp 64−164. (b) Sension, R. J.; Repinec, S. T.; Szarka, A. Z.; Hochstrasser, R. M. *J. Chem. Phys.* **1993**, 98, 6291−6315. (c) Szarka, A. S.; Pugliano, N.; Palit, D. K.; Hochstrasser, R. M. *Chem. Phys. Lett.* **1995**, *240*, 25−30. (d) Saltiel, J.; Waller, A.; Sun, Y.-P.; Sears, D. F. *J. Am. Chem. Soc.* **1990**, *112*, 4580−4581. (e) Saltiel, J.; Waller, A. S.; Sears, D. F. *J. Am. Chem. Soc.* **1993**, *115*, 2453−2465. (f) Petek, H.; Yoshihara, K.; Fujiwara, Y.; Lin, Z.; Penn, J. H.; Frederick, J. H. *J. Phys. Chem.* **1990**, *94*, 7539−7543. (g) Bañares, L.; Heikal, A. A.; Zewail, A. H. *J. Phys. Chem.* **1992**, *96*, 4127−4130.

(3) (a) Allen, M. T.; Whitten, D. G. *Chem. Rev. (Washington, D.C.)* **1989**, *89*, 1691−1702. (b) Morris, D. L.; Gustafson, T. L. *J. Phys. Chem.* **1994**, *98*, 6725−6730. (c) Itoh, T.; Kohler, B. E.; Spangler, C. W. *Spectrochim. Acta, Part A* **1994**, *50*, 2261−2263.

(4) (a) Udayakumar, B. S.; Devadoss, C.; Schuster, G. B. *J. Phys. Chem.* **1993**, *97*, 8713−8717. (b) Ma, J. S.; Dutt, G. B.; Waldeck, D. H.; Zimmt, M. B. *J. Am. Chem. Soc.* **1994**, *116*, 10619−10629. (c) Lenderink, E.; Duppen, K.; Wiersma, D. A. *J. Phys. Chem.* **1995**, *99*, 8972−8977.

(5) (a) Orlandi, G.; Siebrand, W. *Chem. Phys. Lett.* **1975**, *30*, 352−354. (b) Hohlneicher, G.; Dick, B. *J. Photochem.* **1984**, *27*, 215−231. (c) Michl, J.; Klessinger, M. *Excited States and Photochemistry of Organic Molecules*; VCH: New York, 1995; pp 369−372.

(6) (a) Said, M.; Malrieu, J. P. *Chem. Phys. Lett.* **1983**, *102*, 312−316. (b) Hemley, R. J.; Dinur, U.; Vaida, V.; Karplus, M. *J. Am. Chem. Soc.* **1985**, *107*, 836−844. (c) Troe, J.; Weitzel, K.-M. *J. Chem. Phys.* **1988**, *88*, 7030−7039. (d) Negri, F.; Orlandi, G.; Zerbetto, F. *J. Phys. Chem.* **1989**, *93*, 5124−5128.

(7) (a) Bendazzoli, G. L.; Orlandi, G.; Palmieri, P.; Poggi, G. *J. Am. Chem. Soc.* **1978**, *100*, 392−395. (b) Nebot-Gil, I.; Malrieu, J.-P. *Chem. Phys. Lett.* **1981**, *84*, 571−574. (c) Orlandi, G.; Palmieri, P.; Poggi, G. *J. Am. Chem. Soc.* **1979**, *101*, 3492−3497.

(8) (a) Bernardi, F.; De, S.; Olivucci, M.; Robb, M. A. *J. Am. Chem. Soc.* **1990**, *112*, 1737−1744. (b) Bernardi, F.; Olivucci, M.; Robb, M. A. *Acc. Chem. Res* **1990**, *23*, 405−412. (c) Bernardi, F.; Olivucci, M.; Robb, M. A.; Tonachini, G. *J. Am. Chem. Soc.* **1992**, *114*, 5805−5812. (d) Olivucci, M.; Ragazos, I. N.; Bernardi, F.; Robb, M. A. *J. Am. Chem. Soc.* **1993**, *115*, 3710−3721. (e) Celani, P.; Bernardi, F.; Olivucci, M.; Robb, M. A. *J. Chem. Phys.* **1995**, *102*, 5733−5742. (f) Olivucci, M.; Bernardi, F.; Ragazos, I.; Robb, M. A. *J. Am. Chem. Soc.* **1994**, *116*, 1077−1085. (g) Celani, P.; Garavelli, M.; Ottani, S.; Bernardi, F.; Robb, M. A.; Olivucci, M. *J. Am. Chem. Soc.* **1995**, *117*, 11584−11585. (h) Palmer, I. J.; Ragazos, I. N.; Bernardi, F.; Olivucci, M.; Robb, M. A. *J. Am. Chem. Soc.* **1993**, *115*, 673−682. (i) Bearpark, M. J.; Olivucci, M.; Wilsey, S.; Bernardi, F.; Robb, M. A. *J. Am. Chem. Soc.* **1995**, *117*, 6944−6953. (j) Bearpark, M. J.; Bernardi, F.; Clifford, S.; Olivucci, M.; Robb, M. A.; Smith, B. R.; Vreven, T. *J. Am. Chem. Soc.* **1996**, *118*, 169−175. (k) Bearpark, M. J.; Bernardi, F.; Olivucci, M.; Robb, M. A.; Smith, B. R. *J. Am. Chem. Soc.* **1996**, *118*, 5254−5260. (l) Bearpark, M. J.; Bernardi, F.; Olivucci, M.; Robb, M. A.; Clifford, S.; Vreven, T. *Mol. Phys.* **1996**, *89*, 37−46.

(9) A conical intersection is an (n − 2) dimensional subspace of n nuclear coordinates in which two states are degenerate. Movement along the two remaining linearly independent nuclear coordinates (the nonadiabatic coupling and gradient difference vectors) lifts the degeneracy. (a) Teller, E.; *J. Phys. Chem.* **1937**, *41*, 109. (b) Kauzmann, W. *Quantum Chemistry*; Academic Press: New York, 1957; pp 696−697. (c) Herzberg, G.; Longuett-Higgins, H. C. *Discuss. Faraday. Soc.* **1963**, *35*, 77. (d) Herzberg, G. *The Electronic Spectra of Polyatomic Molecules*; Van Nostrand: Princeton, 1966; p 442. (e) Teller, E. *Isr. J. Chem.* **1969**, *7*, 227−235. (f) Longuet-Higgins, H. C. *Proc. R. Soc. London, Ser. A* **1975**, *344*, 147−156. (g) Stone, A. J. *Proc. R. Soc. London, Ser. A* **1976**, *351*, 141−150. (h) Salem, L. *Electrons in Chemical Reactions: First Principles*; Wiley: New York, 1982; pp 148−153. (i) Bonacic-Koutecky, V.; Koutecky, J.; Michl, J. *Angew. Chem., Int. Ed. Engl.* **1987**, *26*, 170−189. (j) Keating, S. P.; Mead, C. A. *J. Chem. Phys.* **1987**, *86*, 2152−2160. (k) Mead, C. A. *Rev. Mod. Phys.* **1992**, *64*, 51−85. (l) Atchity, G. J.; Xantheas, S. S.; Ruedenberg, K. *J. Chem. Phys.* **1991**, *95*, 1862−1876. (m) Manthe, U.; Köppel, H. *J. Chem. Phys.* **1990**, *93*, 1658-1669. (n) Schon, J.; Köppel, H. *J. Chem. Phys.* **1995**, *103*, 9292−9303. (o) Klessinger, M. *Angew. Chem., Int. Ed. Engl.* **1995**, *34*, 549−551. (p) Desouter-Lecomte, M.; Lorquet, J. C. *J. Chem. Phys.* **1977**, *71*, 4391. (q) Michl, J.; Klessinger, M. *Excited States and Photochemistry of Organic Molecules*; VCH: New York, 1995. (r) Michl, J.; Bonacic-Koutecky, V. *Electronic Aspects of Organic Photochemistry*; Wiley: New York, 1990. (s) Gilbert, A.; Baggot, J. *Essentials of Molecular Photochemistry*; Blackwell: London, 1991.

(10) (a) Michl, J. *Pure Appl. Chem.* **1975**, *41*, 507−534. (b) Gerhartz, W.; Poshusta, R. D.; Michl, J. *J. Am. Chem. Soc.* **1976**, *98*, 6427−6443. (c) Gerhartz, W.; Poshusta, R. D.; Michl, J. *J. Am. Chem. Soc.* **1977**, *99*, 4263−4271.

(11) Van der Lugt, W. T. A. M.; Oosterhoff, L. J. *J. Am. Chem. Soc.* **1969**, *91*, 6042.

(12) (a) Rockley, M. G.; Salisbury, K. *J. Chem. Soc., Perkin Trans. 2* **1973**, 1582−1585. (b) Steer, R. P.; Swords, M. D.; Crosby, P. M.; Phillips, D.; Salisbury, K. *Chem. Phys. Lett.* **1976**, *43*, 461−464. (c) Ghiggino, K. P.; Phillips, D.; Salisbury, K.; Swords, M. D. *J. Photochem.* **1977**, *7*, 141−146. (d) Ghiggino, K. P.; Hara, K.; Salisbury, K.; Philips, D. *J. Photochem.* **1978**, *8*, 267−271. (e) Ghiggino, K. P.; Hara, K.; Mant, G. R.; Phillips, D.; Salisbury, K.; Steer, R. P.; Swords, M. D. *J. Chem. Soc., Perkin Trans. 2* **1978**, 88−91. (f) Crosby, P. M.; Dyke, J. M.; Metcalfe, J.; Rest, A. J.; Salisbury, K.; Sodeau, J. R. *J. Chem. Soc., Perkin Trans. 2* **1977**, 182−185.

(13) (a) Lyons, A. L.; Turro, N. J. *J. Am. Chem. Soc.* **1978**, *100*, 3177−3181. (b) Condirston, D. A.; Laposa, J. D. *Chem. Phys. Lett.* **1979**, *63*, 313−317. (c) Bonneau, R. *J. Am. Chem. Soc.* **1982**, *104*, 2921−2923.

(14) (a) Hollas, J. M.; Ridley, T. *J. Mol. Spectrosc.* **1981**, *89*, 232−253. (b) Hollas, J. M.; Musa, H.; Ridley, T.; Turner, P. H.; Weisenberger, K. H.; Fawcett, V. *J. Mol. Spectrosc.* **1982**, *94*, 437−455. (c) Syage, J. A.; Al Adel, F.; Zewail, A. H. *Chem. Phys. Lett.* **1983**, *103*, 15−22. (d) Seeman, J. I.; Grassian, V. H.; Bernstein, E. R. *J. Am. Chem. Soc.* **1988**, *110*, 8542−8543. (e) Grassian, V. H.; Bernstein, E. R.; Secor, H. V.; Seeman, J. I. *J. Phys. Chem.* **1989**, *93*, 3470−3474. (f) Condirston, D. A.; Laposa, J. D. *J. Lumin.* **1978**, *16*, 47−59.

(15) (a) Hemley, R. J.; Leopold, D. G.; Vaida, V.; Karplus, M. *J. Chem. Phys.* **1985**, *82*, 5379−5397. (b) Zeigler, L. D.; Varotsis, C. *Chem. Phys. Lett.* **1986**, *123*, 175−181. (c) Hemley, R. J.; Leopold, D. G.; Vaida, V.; Roebber, J. L. *J. Phys. Chem.* **1981**, *85*, 134−135. (d) Leopold, D. G.; Hemley, R. J.; Vaida, V.; Roebber, J. L. *J. Chem. Phys.* **1981**, *75*, 4758−4769.

(16) Swiderek, P.; Fraser, M.-J.; Michaud, M.; Sanche, L. *J. Chem. Phys.* **1994**, *100*, 70−77.

(17) Hui, M. H.; Rice, S. A. *J. Chem. Phys.* **1974**, *61*, 833−842.

(18) (a) Drescher, W.; Kendler, S.; Zilberg, S.; Zingher, E.; Zuckermann, H.; Haas, Y. I. *J. Chem. Phys.* **1994**, *101*, 11082−11083. (b) Zilberg, S.; Haas, Y. *J. Chem. Phys.* **1995**, *103*, 20−36.

(19) Smith, B. R.; Bearpark, M. J.; Robb, M. A.; Bernardi, F.; Olivucci, M.; *Chem. Phys. Lett.* **1995**, *242*, 27−32.

(20) (a) Bernardi, F.; Olivucci, M.; Robb, M. A. *J. Am. Chem. Soc.* **1992**, *114*, 1606−1616. (b) Bearpark, M. J.; Bernardi, F.; Olivucci, M.; Robb, M. A. *Chem. Phys. Lett.* **1994**, *217*, 513−519.

(21) Kendler, S.; Zilberg, S.; Haas, Y. *Chem. Phys. Lett.* **1995**, *242*, 139−146.

(22) Heckman, R. C. *J. Mol. Spectrosc.* **1958**, *2*, 27.

(23) (a) Harrigan, E. T.; Hirota, N. *Chem. Phys. Lett.* **1973**, *22*, 29. (b) Brocklehurst, B.; Tawn, D. N. *Spectrochim. Acta, Part A* **1974**, *30*, 1807. (c) Harrigan, E. T.; Hirota, N. *J. Am. Chem. Soc.* **1975**, *97*, 6647.

(24) Byrne, J. P.; Ross, I. G. *Aust. J. Chem.* **1971**, *24*, 1107.

(25) Suarez, M. L.; Duguid, R. J.; Morrison, H. *J. Am. Chem. Soc.* **1989**, *111*, 6384−6391.

(26) Allinger, N. L. *Adv. Phys. Org. Chem.* **1976**, *13*, 1.

(27) (a) Anderson, P. W. *Phys. Rev.* **1959**, *115*, 2. (b) Said, M.; Maynau, D.; Malrieu, J.-P.; Bach, M.-A. G. *J. Am. Chem. Soc.* **1984**, *106*, 571−579. (c) Said, M.; Maynau, D.; Malrieu, J.-P. *J. Am. Chem. Soc.* **1984**, *106*, 580−587. (d) Durand, P.; Malrieu, J.-P. *Adv. Chem. Phys.* **1987**, *67*, 321−412.

(28) (a) Ragazos, I. N.; Robb, M. A.; Bernardi, F.; Olivucci, M. *Chem. Phys. Lett.* **1992**, *197*, 217−223. (b) Bearpark, M. J.; Robb, M. A.; Schlegel, H. B. *Chem. Phys. Lett.* **1994**, *223*, 269−274.

(29) Frisch, M. J.; Trucks, G. W.; Schlegel, H. B.; Gill, P. M. W.; Johnson, B. G.; Robb, M. A.; Cheeseman, J. R.; Keith, T. A.; Petersson, G. A.; Montgomery, J. A.; Raghavachari, K.; Al-Laham, M. A.; Zakrzewski, V. G.; Ortiz, J. V.; Foresman, J. B.; Cioslowski, J.; Stefanov, B. B.; Nanayakkara, A.; Challacombe, M.; Peng, C. Y.; Ayala, P. Y.; Chen, W.; Wong, M. W.; Andres, J. L.; Reploge, E. S.; Gomperts, R.; Martin, R. L.; Fox, D. J.; Binkley, J. S.; Defrees, D. J.; Baker, J.; Stewart, J. P.; Head-Gordon, M.; Gonzales, C.; Pople, J. A. *Gaussian 94*; Gaussian, Inc.: Pittsburgh, 1995.

(30) Yamamoto, N.; Vreven, T.; Robb, M. A.; Frisch, M. J.; Schlegel H. B. *Chem. Phys. Lett.* **1996** , *250*, 373−378.

(31) (a) Unett, D. J.; Caldwell, R. A. *Res. Chem. Intermed.* **1995**, *21*, 665−709. (b) Ni, T.; Caldwell, R. A.; Melton, L. A. *J. Am. Chem. Soc.* **1989**, *111*, 457−464. (c) Caldwell, R. A.; Jacobs, L. D.; Furlani, T. R.; Nalley, E. A.; Laboy, J. *J. Am. Chem. Soc.* **1992**, *114*, 1623−1625. (d) Arai, T.; Tokumaru, K. *Chem. Rev. (Washington, D.C.)* **1993**, *93*, 23. (e) Bonneau, R.; Herran, B. *Laser Chem.* **1984**, *4*, 151−170. (f) Bonneau, R. *J. Photochem.* **1979**, *10*, 439−449. (g) Görner, H. *J. Phys. Chem.* **1989**, *93*, 1826−1832.

(32) Wagner, B. D.; Szymanski, M.; Steer, R. P. *J. Chem. Phys.* **1993**, *98*, 301−307.

(33) Zimmerman, H. E.; Kamm, K. S.; Werthermann, D. P. *J. Am. Chem. Soc.* **1975**, *97*, 3718−3725.